

# The structure of gallery networks in the nests of termite *Cubitermes* spp. revealed by X-ray tomography

Andrea Perna · Christian Jost · Etienne Couturier ·  
Sergi Valverde · Stéphane Douady · Guy Theraulaz

Received: 9 March 2007 / Revised: 4 April 2008 / Accepted: 4 April 2008  
© Springer-Verlag 2008

**Abstract** Recent studies have introduced computer tomography (CT) as a tool for the visualisation and characterisation of insect architectures. Here, we use CT to map the three-dimensional networks of galleries inside *Cubitermes* nests in order to analyse them with tools from graph theory. The structure of these networks indicates that connections inside the nest are rearranged during the whole nest life. The functional analysis reveals that the final network topology represents an excellent compromise between efficient connectivity inside the nest and defence against attacking predators. We further discuss and illustrate the usefulness of CT to disentangle environmental and specific influences on nest architecture.

**Keywords** *Cubitermes* nests · Computer tomography · Networks · Social insects · Animal architectures · Termite mounds

---

**Electronic supplementary material** The online version of this article (doi:10.1007/s00114-008-0388-6) contains supplementary material, which is available to authorized users.

---

A. Perna (✉) · C. Jost · S. Valverde · G. Theraulaz  
Centre de Recherches sur la Cognition Animale,  
CNRS UMR 5169, Université Paul Sabatier,  
118 route de Narbonne, 31062 Toulouse Cedex 9, France  
e-mail: perna@cict.fr

E. Couturier · S. Douady  
Laboratoire Matière et Systèmes Complexes (MSC),  
UMR 7057 CNRS & Université Paris Diderot,  
Bâtiment Condorcet CC7056, 75205 Paris CEDEX 13, France

S. Valverde  
ICREA-Complex Systems Lab, Universitat Pompeu Fabra,  
Dr. Aiguader 80, 08003 Barcelona, Spain

## Introduction

Termite nests are among the most amazing animal-built structures. They attain sizes two to four orders of magnitude above the size of the individuals that build them (Grassé 1984). In addition, they do not simply result from the repetition of local patterns, but present a coherent global organisation. More generally, the nest architecture contributes to maintain homeostasis of the local environment (Lüscher 1955; Korb and Linsenmair 1999, 2000; Korb 2003; see also Turner 2000 for a review) and plays an important role in defence from predators (Grassé 1984; Dejean and Ruelle 1995; Dejean et al. 1996, 1997). Furthermore, being the site of most colony activities, the form of nests is also likely to affect spatial distribution, task repartition (Franks and Tofts 1994; Traniello and Rosengaus 1997) and spreading of illnesses inside a colony (Pie et al. 2004).

In order to understand how these functions are related to the characteristics of the nests, it is necessary to find appropriate and functionally relevant descriptors of the different nest structures. For instance, the volume, surface area and number of different elements in a nest provide indirect information on the size and age of a colony. However, they are not sufficient to account for most of the biological functions of the nests, which are more likely to depend on parameters like the form, the relative position and the arrangement of nest elements, in other words, on the *inter-relations* between the different parts. One of the most powerful simplifications to represent systems with interconnected subunits are graphs. Graph representations have been used especially in the past few years to characterise a variety of systems, ranging from patterns of streets in a town (Buhl et al. 2006b; Porta et al. 2006; Gastner

and Newman 2006) to the arrangement of servers on the Internet (Albert et al. 2000) and the branching patterns of rivers (Horton 1945; Strahler 1952). A graph representation gives access to the tools developed in the field of graph theory to analyze the functions of transport and exchange of information or material that are shared by such different systems.

Recently, Buhl et al. (2004) have used a graph representation to characterise the complex galleries dug by ants in laboratory conditions. By computing some basic properties of the graphs that describe the ant galleries, these authors were able to associate each gallery system to a set of functional indicators, like the efficiency of transportation across different parts of the network and the robustness against the accidental occlusion of some branches of the network. The experimental setup used in their experiment, however, was quite artificial, with ants confined to dig in a bidimensional horizontal layer, while natural nests are dug in a three-dimensional (3-D) environment. For this reason, the biological significance of the different indicators was difficult to assess.

Following the same line of research, the aim of the present paper is to test the potential applications of tools of graph theory to infer functional properties of the network of chambers and galleries inside the nests built by social insects. In order to do that, we map the whole network of galleries inside nests built by African termites of the genus *Cubitermes* under natural conditions.

Mapping the whole system of galleries inside a termite nest is a technically difficult task that, to our knowledge, has never been performed before. In fact, in order for the representation to be meaningful, *all* the chambers in the nest must be individually identified and their connections mapped.

Various techniques have successfully been used to characterise termite nests and similar architectures produced by social insects. These range from step-by-step excavation and measurements (Tschinkel 1998, 1999a, b; Mikheyev and Tschinkel 2004) to radiographies (see, e.g., Desneux 1956) and to casting by injecting orthodontic plaster or similar substances into the galleries (Williams and Lofgren 1988; Tschinkel 2004; Mikheyev and Tschinkel 2004). However, with all these techniques, the task of visualizing or measuring inner parts of the nests remains a difficult one.

Recent studies have introduced computer tomography (CT) as a promising tool for the visualisation and characterisation of social insect nests and other animal-built architectures (Hervier et al. 2001; Fuchs et al. 2004; Halley et al. 2005). CT only requires that the structures can be transported and passed intact

through the scanner. Among the advantages offered by CT are those of being nondestructive (repeated measures of the same structure are possible even on active nests) and quantitative (conventional CT instruments achieve a spatial resolution of about 0.5 mm). In addition, it produces digital data that can be processed quickly, which is necessary when the entire nest must be processed (for instance, to extract the network) or to characterise complex forms.

This technique allowed us to measure several indicators of the size and form of nest structures (for which only qualitative descriptions were available) and to map for the first time the whole connectivity network of six *Cubitermes* nests. Some characteristics of these networks, like the connectivity and the distribution of connections inside the nest are of crucial biological interest because of their impact on termite communication and defence.

## Methods

### Nests, X-ray tomography and preprocessing

Six *Cubitermes* spp. nests were used in the analysis. Two nests, henceforth labelled M9 and M18, came from a savannah-type region in the Central African Republic. The other nests (M10, M11, M12 and M19) came from different equatorial forest regions in the Central African Republic and Cameroon. Nest M12 was built by *Cubitermes fungifaber*. The exact species that built the other nests are not known. All the nests belong to private or public collections (Natural History Museums of Paris and Toulouse).

Each nest was imaged using X-ray tomography with a medical scanner and reconstructed into a series of virtual cuts (thickness 1 mm, 512 × 512 pixels).

### Analysis

The “dicom” file format images issued from the scanner were merged into a single 3-D volume with binary information (wall material or empty space). The subsequent analysis was performed with a dedicated software that can be requested from the authors. Here, we summarise the major steps of the analysis. A more technical description is provided in [ESM](#).

Chambers are identified with a sort of “watershed algorithm,” by detecting image regions far from (internal and external) nest walls (more than about 1.5 mm). Given the narrow diameter of the corridors (less than ~ 0.5 mm in radius), these regions either belong to a chamber or to the space outside the nest, but never to

a corridor. The thus identified chamber cores are numbered and dilated to progressively fill the whole empty space. When two chambers have grown enough to fill about half of the corridors from both sides, adjacent chambers get in touch. At this moment, the software marks the existence of a connection between them. The same chamber dilation is then repeated, but this time, growth is allowed through the nest walls. When two different chambers get in touch, they are marked as adjacent. The results of this automatic segmentation were verified and corrected by hand. We corrected in particular for spurious corridors that had been marked for nest M9, where a few straws passing through the nest had been erroneously marked as corridors. With this only exception, the technique gave reliable results.

For each chamber, the principal axes of orientation were estimated by performing a principal component analysis on the coordinates of all the voxels belonging to the chamber (a voxel is the 3-D equivalent of a pixel). We define chamber elongation  $\ell = \sqrt{\lambda_{\min}/\lambda_{\max}}$  where  $\lambda_{\max}$  and  $\lambda_{\min}$  are the maximum and minimum eigenvalues associated to the principal components, respectively. This provides a quantification of shape elongation that is robust to noise and normalised in the interval 0–1. It is also invariant to translation, scaling and rotation.

We also estimated the volume and the surface area of each chamber. The volume was estimated by counting the total number of voxels inside a chamber and multiplying it by the volume of the voxel. The surface was estimated as described in Lang et al. (2001). As an estimator of compactness, we computed the isoperimetric quotient that expresses in 3-D the ratio of the volume of an object to the volume of a sphere with the same surface. Given a volume  $V$  and a surface area  $S$ , the isoperimetric quotient is computed as  $36\pi V^2/S^3$ . This parameter is bounded in the interval 0–1 and is equal to 1 for a sphere.

In all nests, chambers and corridors formed at least one big connected network where each chamber can be reached from any other chamber, but we also found some isolated chambers. These were excluded from the network analysis since only connected chambers were accessible to termites when the nest was active and because certain network properties are not defined for disconnected networks.

We used a standard algorithm (Dijkstra 1959) to compute the characteristic path length of the network (this is a measure of topological distance, indicating the minimum number of corridors to cross when going from any chamber to any other chamber of the nest). Node degree for each chamber is defined as the number of corridors opening on that chamber. We computed the

“fraction of connected adjacencies” for each chamber as the ratio between the number of connected chambers and the total number of adjacent chambers. Chambers that had no adjacency point to the nest wall (“central chambers”) were marked differently from those that were right below the external nest surface (“peripheral chambers”).

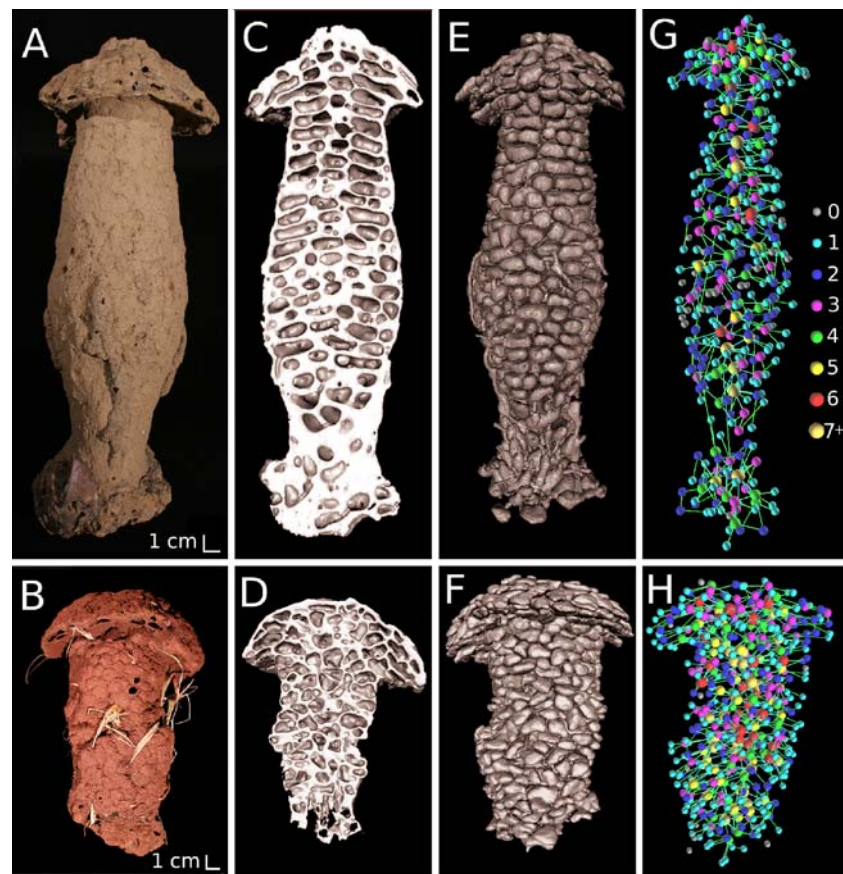
In the absence of precise taxonomic information for five out of six nests, our analysis will concern the functional properties of the genus *Cubitermes* in general. However, we know for each nest whether it comes from a savannah or a forest region, which permits to compare the nest characteristics with respect to this origin. All statistical tests use a significance level of  $\alpha = 0.05$  and are performed with the R software (R Development Core Team 2006). The chambers in the cap and in the base will be omitted in these comparisons because the former vary in number with the number of caps and the latter can be incomplete.

## Results

### Qualitative description

The analysed nests consisted in general of a single column covered by a single cap (see Fig. 1), with the exception of M11 (which had three caps and a second small column) and M19 (which had no cap). The appearance of this latter nest suggests that it was still under construction when it was collected. In this nest, the lower part had a similar structure to the one observed in the other nests. The upper part – the one of more recent construction – presented big, irregular chambers, from which a series of vertical corridors departed (arranged like palisades). These corridors ran up to the top of the nest but did not open on the exterior of the nest. Apart from these differences, the nest was in perfect condition and all the fine structures were clearly observable and identifiable. The peculiar traits of this nest are therefore not artifacts due to bad nest conservation or erosion (that act on the nest from *outside* and whose effect should be more primarily evident on the external nest surface), but are likely due to the fact that it was under construction. Forest nests M10, M11, M12 and M19 had a similar general aspect and a similar ratio of height over diameter; the two nests collected in the savannah (M9 and M18) were more compact and had less regularly arranged chambers. Figure 1 shows pictures of nests M10 (top row) and M9 (bottom row), a tomographic cut of the same nests and a virtual cast, where only the empty space inside the nest is represented (chambers and galleries).

**Fig. 1** Analysis of nest M10 (top row, from a forest) and nest M9 (bottom row, from a savannah): **a, b** pictures of the nests; **c, d** a tomographical cut of the same nests; **e, f** a virtual “cast” of the chambers and galleries; **g, h** a representation of chambers and galleries as a network, where each node corresponds to a chamber in the original nest and each edge to a corridor. The colour of the nodes reflects their degree, i.e. the number of corridors connected to that chamber (see legend in **g**)



The gallery system is also schematically represented as a network, where each chamber is marked by a node and a corridor by an edge. The colour and size of the node reflect its degree, that is the number of corridors opening on the chamber.

#### The network of galleries

The chambers are tightly packed inside the nest, with each chamber having on average about 10 adjacent chambers (see Table 1). Since, in general, no long-distance connections are observed (the only exception being the corridors built on the external nest surface in M10), a chamber will be able to establish, at most, an average of 10 connections.

However, the number of 2.5 corridors observed on average for each chamber (“node degree” in Table 1) is much lower than this theoretical limit, suggesting that physical packaging of the chambers is not the main factor limiting the number of connections between chambers. Simple mathematical reasoning tells that one necessary condition for a graph with  $N$  nodes to be connected is that of having at least  $N - 1$  edges. This means that the average node degree of a connected

network cannot be less than  $\sim 2$ . *Cubitermes* networks of galleries are much closer to this minimum value than to the maximum value of 10, suggesting that these networks tend to minimise, not to maximise, connectivity.

The low average node degree of the gallery system leads to networks where the number of connections is barely sufficient for each node to be reachable from every other node. Indeed, the obstruction of a single corridor is sufficient in more than 40% of the cases to make the network disconnected (Table 1). This is exemplified in Fig. 2a where the same network as in Fig. 1g has been stretched to better illustrate that point (but keeping exactly the same topological arrangement of nodes and edges). In the figure, the nodes and edges whose removal leads to network disconnection are represented in light colour.

Physical packaging constraints predict that peripheral chambers (being defined as chambers adjacent to the external nest wall) should have lower connectivity simply because they have fewer neighbours to connect to. Lower connectivity of peripheral chambers is indeed observed. However, the lower number of neighbours is not sufficient to account for it. This is shown in Fig. 2b, where the number of connections established

**Table 1** Measures of relevant nest parameters

Property	M9 (savannah)	M18 (savannah)	M10 (Forest)	M11 (Forest)	M12 (Forest)	M19 (Forest)
Height (cm)	18	18	29	31	33	33
Maximum diameter (without cap, cm)	7.0	7.2	8.5	4.8 × 2	7.2	8.5
Total volume (cm <sup>3</sup> )	764	571	1147	1792	622	1174
Total volume of the chambers (cm <sup>3</sup> )	319	234	416	569	322	523
Number of chambers	532	312	396	344	190	295
Mean volume of the chambers ± SEM (cm <sup>3</sup> )	0.599 ± 0.014	0.751 ± 0.026	1.052 ± 0.035	1.655 ± 0.063	1.697 ± 0.069	1.774 ± 0.068
Mean surface of the chambers ± SEM (cm <sup>2</sup> )	4.54 ± 0.09	5.44 ± 0.15	6.38 ± 0.18	9.24 ± 0.28	9.73 ± 0.35	9.40 ± 0.30
Chamber isoperimetric quotient ± SEM	0.461 ± 0.006	0.424 ± 0.009	0.484 ± 0.008	0.403 ± 0.009	0.406 ± 0.010	0.405 ± 0.007
Chamber elongation ( $\ell$ ) ± SEM	0.434 ± 0.006	0.435 ± 0.008	0.417 ± 0.007	0.397 ± 0.008	0.389 ± 0.010	0.407 ± 0.007
Built/empty space	1.40	1.44	1.75	2.15	0.93	1.24
Angle from vertical $\theta$ (median deg, 1 <sup>st</sup> –3 <sup>rd</sup> quartile)	34 (22–52)	39 (23–63)	24 (16–47)	26 (16–40)	14(9–25)	29 (17–69)
Radial direction of higher slope $\alpha$ (mean deg ± AD)	0 ± 73	–10 ± 77	2 ± 70	4 ± 75	–12 ± 70	2 ± 72
Connected component of the network (nodes)	507	287	349	260	183	268
Number of chambers adjacent to a given chamber (mean ± SEM)	11.15 ± 0.19	10.16 ± 0.26	8.90 ± 0.20	9.18 ± 0.26	9.82 ± 0.26	9.35 ± 0.22
Node degree (mean ± SEM)	2.67 ± 0.08	2.39 ± 0.10	2.06 ± 0.07	2.15 ± 0.10	2.55 ± 0.13	3.27 ± 0.14
Fracture of edges whose removal leads to network fragmentation	0.36	0.44	0.73	0.65	0.36	0.17

SEM standard error of the mean, AD mean angular deviation

by a chamber is normalised over the number of neighbours of that chamber. Differences between central and peripheral chambers are statistically significant [two-way ANOVA of the arcsine transformed fractions of connected chambers on nest (block factor) and position ( $F_{2051,1} = 70.5, p < 0.001$ )], and the difference depended on the nest (interaction,  $F_{2051,5} = 4.04, p = 0.001$ ).

Figure 2c reports the degree distribution of the network. This corresponds to the percent of chambers having  $k$  connected corridors plotted vs  $k$ . The distribution is exponential, with many chambers having a single connection and very few chambers having seven or more connections.

However, it has to be noticed that the average node degree is not equal in all nests. In particular, it is significantly higher in nest M19 (the nest that appears to be under construction) than in the other nests (two sample Mann–Whitney test on node degree  $W = 319149, n = (295, 1774), p < 0.001$ ).

The length of the paths between nodes also depends on network sparseness, because with fewer connections available, the distance one has to travel on average in order to go from one point to the other becomes longer. In Fig. 2d, we report the distribution of the lengths of the paths connecting any two nodes in the observed networks and – for comparison – the minimum possible distribution that we would have if all adjacent chambers were interconnected.

### Chambers and corridors

As a side result, CT analysis also allowed us to quantify the size and form of some nest structures for which the literature only provides qualitative descriptions. Most of these measures are reported in Table 1. The nests differ in size and have different numbers of chambers. In particular, a nested ANOVA on the volume of the chambers with repeated measures for chambers in the same nest reveals significant differences between forest and savannah nests ( $F_{4,1} = 10.03, p = 0.03$ ). The chambers of the two nests collected in the savannah have smaller volumes.

In spite of differences in size, the chambers from all the nests have similar values for parameters that concern the form. Chamber surface is strongly correlated with chamber volume ( $r = 0.98$ ). Accordingly, the isoperimetric quotients of the chambers (a descriptor of form) is comprised in a narrow range from 0.4 to 0.5 on average in all nests (Table 1), and a repeated-measure nested ANOVA on this parameter does not show any difference between savannah and forest nests ( $F_{4,1} = 0.27, p = 0.63$ ).

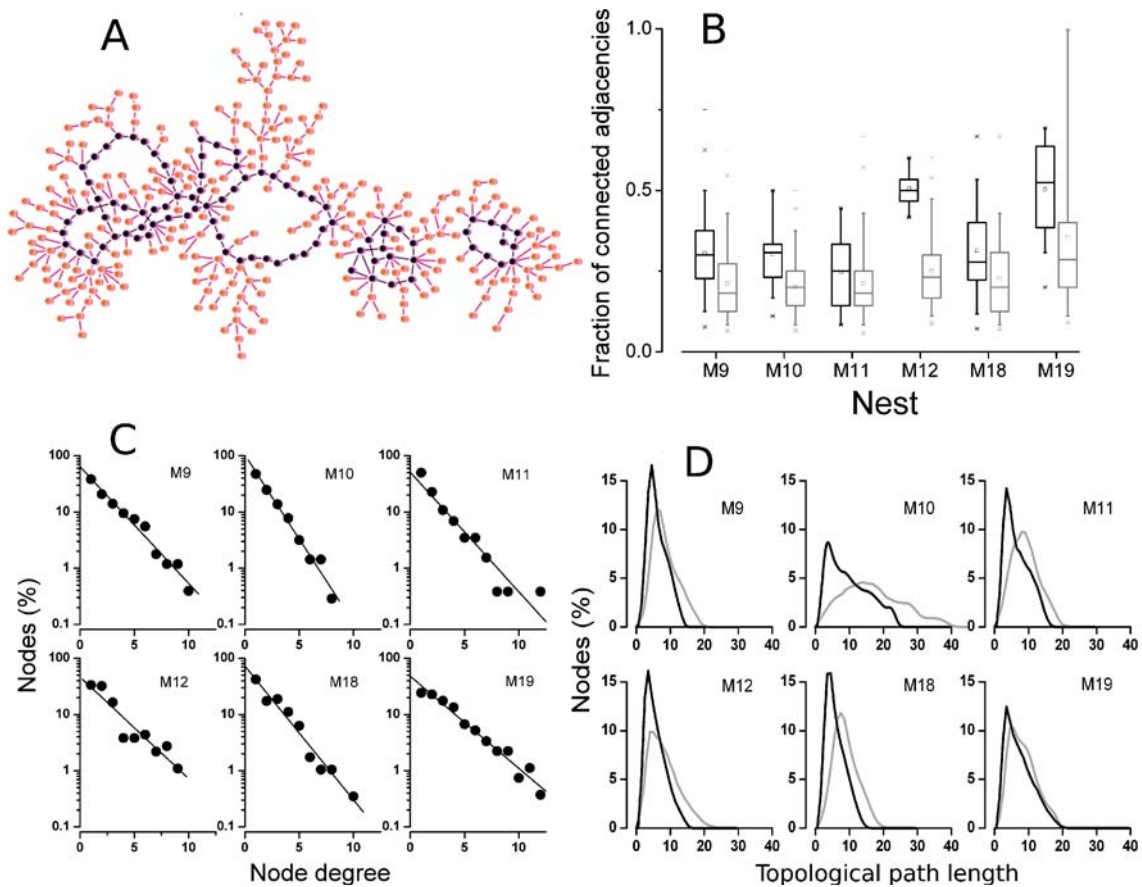


**Fig. 2** **a** The same network as in Fig. 1g in a flat representation to show the topological arrangement of nodes (interconnected chambers). The edges whose removal leads to network disconnection are represented in *lighter colour*. **b** Fraction of adjacent chambers to a given chamber that are physically connected to it with a corridor. *Black*: central chambers. *Gray*: peripheral chambers. **c** Node degree distribution, that is the number of

chambers as a function of the number of corridors connected to them. The *line* represents an exponential fit to the data. **d** Distribution of path lengths in the six nests for the observed network of galleries (*gray curve*) and theoretical distribution that would be obtained if all adjacent chambers were connected (*black curve*)

The chambers present an inclination of about 30 degrees (angle  $\theta$  in Table 1 and Fig. S2 in ESM) and savannah nests have more inclined chambers ( $F_{4,1} = 13.43$ ,  $p = 0.02$ ). The direction of maximal slope (angle  $\alpha$  in Table 1) is strongly oriented along the radial axis, mounting from the periphery of the nest toward the centre in all nests. Values of this angle close to 180 degrees are to be expected for chambers whose higher side was on the peripheral part of the nest, while the observed values of this angle near zero indicate that the chamber floor is higher toward the centre of the nest.

## Discussion

The description of *Cubitermes* nests that we obtained with X-ray tomography offers one of the first detailed quantitative characterisations of termite constructions.

In all nests, the connections between chambers are much less frequent than would be possible based on physical constraints. In any connectivity network, low connectivity is typically – and intuitively – associated with increased average distances and higher traffic on the corridors.

However, it is likely that the sparseness of these networks offers advantages for nest defence. It is known that *Cubitermes subarquatus* soldiers defend the entrance of exposed galleries when the nest is attacked by ants (Dejean and Féron 1999). It is also speculated that the size of the corridors, just slightly bigger than the size of a soldier, constitutes an adaptation facilitating defence in similar circumstances.

Here, we argue that not just the size of the corridors, but the arrangement of the whole gallery network provides benefits for defence. The low connectivity easily permits isolating attacked parts of the nest by closing

a single corridor (plugging galleries with liquid earth is also a reported defence strategy for termites of the *Cubitermes* genus; Dejean and Fénéron 1999). If so, one would expect an advantage if the connectivity is not evenly distributed inside the nest. In particular, peripheral chambers should be less connected, because these are more exposed to attacks by other insects. This is exactly what is found in these nests. Lower connectivity of peripheral chambers was also reported for *Noditermes* nests by Iniesto et al. (2001), and it could be a common feature of many epigeous nests of Termitinae.

As mentioned above, weak connectivity is usually associated with increased path length. Surprisingly, the characteristic path length distribution in our nests is very close to the one that could be achieved under maximal connectivity (Fig. 2d). *Cubitermes* seem to have found a very good compromise between optimising traffic flow and defence.

The degree of network nodes follows an exponential decay distribution in all nests (Fig. 2c). Interestingly, an exponential distribution of node degree is also observed for networks of galleries dug by *Messor sanctus* ants in an artificial setup (Buhl et al. 2006a). Many nests built under natural conditions also exhibit an exponential decay of the density of nest elements with respect to depth (Tschinkel 2004; Mikheyev and Tschinkel 2004). Together, these observations suggest that an exponential degree distribution could be a recurrent feature of gallery networks of insects. Growth models where new elements are added with uniform probability to pre-existing elements can generate networks with exponential degree distribution (Albert and Barabasi 2002; Buhl et al. 2006a). However, the structure of *Cubitermes* networks gives us indications that the final topology of galleries inside these nests is not simply the result of additive growth, but must also involve rearrangements of existing connections and removal of superfluous connections. It is known that, in *Cubitermes* nests, new chambers can only be added at the top and are never rearranged (Noirot and Noirot-Timothee 1962). On the contrary, from the map of the internal transportation network that we have obtained, it emerges that corridors are rearranged (opened and closed) during nest life:

1. There exist connections between the two columns of nest M11. In nests composed of more columns, additional columns are added at subsequent times. Connections linking chambers in different columns consequently must have been dug after the completion of the first column.
2. In all the nests, we observe the presence of a small number of disconnected chambers. Termites must have had access to these chambers during construction, and the corridors connecting to them must have been closed later on.
3. Nest M19, which is apparently still under construction, has a significantly higher connectivity than all the other nests. This indicates that some corridors are removed in order to achieve the final topology.

One possibility is that, in a first phase of nest construction, termites realise a higher number of connections between the chambers; then, connections where less traffic flows would be progressively removed. This would lead to networks with weak connectivity, keeping, at the same time, displacement paths short, as is actually observed. Direct observation and field work will be required to test this possibility.

The high spatial resolution offered by CT allows us to quantify a variety of other descriptive parameters of the nests. In the present paper, we were able to measure the surface, volume, orientation and some descriptors of the form of individual chambers. We found that size and orientation of chambers change significantly between nests from different environments (forest or savanna). Some characteristics, however, are common to all the nests. These include the isoperimetric quotient of the chambers, the centrifugal direction of chambers slope and many network parameters, like the particular degree distribution and the low network connectivity. The relative constancy of these features across all nests suggests that they could be a byproduct of an overall design algorithm. On the contrary, features that vary in the different environments could represent a particular adaptation to the local conditions. The presented techniques combined with future field work that provides precise taxonomic information could help to disentangle the specific from the environmental factors that influence nest architecture, while also giving clues about the underlying behavioural mechanisms.

To summarise, we found that termites of the genus *Cubitermes* build nests with a network of connected chambers that represent an excellent compromise between connectivity inside the nest and defence against attacking predators. The used techniques of CT and graph theory offer new perspectives to gain further understanding of the functioning of these colonies.

**Acknowledgements** We thank JP Suzzoni (Université Toulouse III), P Annoyer (Museum of Natural History, Toulouse) and A Nel (National Museum of Natural History,

Paris) for lending the nests and F Joffre (CHU Rangueil, Toulouse) for giving us access to the hospital tomography scanner. We also would like to thank G Malandain (Inria, Sophia Antipolis) for sharing code that was used in the analysis and D Legland (Inra, Nantes) for help with formulae to estimate chamber surface area. A Perna is supported by a grant from the *Ambassade de France* in Rome and the Italian *Ministero degli Affari Esteri*. This work was supported by ANR-06-BYOS-0008.

## References

- Albert R, Barabasi A (2002) Statistical mechanics of complex networks. *Rev Mod Phys* 74(47):47–97
- Albert R, Jeong H, Barabasi A (2000) Error and attack tolerance of complex networks. *Nature* 406(6794):378–382
- Buhl J, Gautrais J, Solé R, Kuntz P, Valverde S, Deneubourg JL, Theraulaz G (2004) Efficiency and robustness in ant networks of galleries. *Eur Phys J B* 42(1):123–129
- Buhl J, Gautrais J, Deneubourg JL, Kuntz P, Theraulaz G (2006a) The growth and form of tunnelling networks in ants. *J Theor Biol* 243(3):287–298
- Buhl J, Gautrais J, Reeves N, Solé R, Valverde S, Kuntz P, Theraulaz G (2006b). Topological patterns in street networks of self-organized urban settlements. *Eur Phys J B* 49(4):513–522.
- Dejean A, Féneron R (1999) Predatory behaviour in the ponerine ant, *Centromyrmex bequaerti*: a case of termitolesty. *Behav Processes* 47:125–133
- Dejean A, Ruelle JE (1995) Importance of *Cubitermes* termitaries as helter for alien incipient termite societies. *Insectes Soc* 42:129–136
- Dejean A, Bolton B, Durand J (1997) *Cubitermes subarquatus* termitaries as shelters for soil fauna in african rainforests. *J Nat Hist* 31(8):1289–1302
- Dejean A, Durand J, Bolton B (1996) Ants inhabiting *Cubitermes* termitaries in african rain forests. *Biotropica* 28(4):701–713
- Desneux J (1956) Structures “atypiques” dans les nidifications souterraines d’*Apicotermes lamani* SJ. (Isoptera, termitidae), mises en évidence par la radiographie. *Insectes Soc* 3(2):277–281
- Dijkstra EW (1959) A note on two problems in connexion with graphs. *Numer Math* 1:269–271
- Franks NR, Tofts C (1994) Foraging for work: how tasks allocate workers. *Anim Behav* 48:470–472
- Fuchs A, Schreyer A, Feuerbach S, Korb J (2004) A new technique for termite monitoring using computer tomography and endoscopy. *Int J Pest Manag* 50(1):63–66
- Gastner MT, Newman MEJ (2006) Optimal design of spatial distribution networks. *Phys Rev E* 74:016117
- Grassé PP (1984) *Termitologia*, tome 2: fondation des sociétés, construction. Masson, Paris
- Halley JD, Burd M, Wells P (2005) Excavation and architecture of Argentine ant nests. *Insectes Soc* 52:350–356
- Hervier B, Josens G, Deligne J, Terwinghe E, Verbanck J (2001) Etude des structures internes des nids de termites par analyse d’image. *Actes Colloq Insectes Soc* 14:45–49
- Horton RE (1945) Erosional development of streams and their drainage basins: hydrophysical approach to quantitative morphology. *Geol Soc Am Bull* 56:275–370
- Iniesto P, Deligne J, Josens G, Verbanck J (2001) Morphologie fonctionnelle des nids de *Noditermes aburiensis* (insecta isoptera). *Actes Colloq Insectes Soc* 14:39–43
- Korb J (2003) Thermoregulation and ventilation of termite mounds. *Naturwissenschaften* 90(5):212–219
- Korb J, Linsenmair K (1999) The architecture of termite mounds: a result of a trade-off between thermoregulation and gas exchange? *Behav Ecol* 10(3):312–316
- Korb J, Linsenmair K (2000) Ventilation of termite mounds: new results require a new model. *Behav Ecol* 11(5):486–494
- Lang C, Ohser J, Hilfer R (2001) On the analysis of spatial binary images. *J Microsc* 203:303–313
- Lüscher M (1955) Der Sauerstoffverbrauch bei Termiten und die Ventilation des Nestes bei *Macrotermes natalensis* (haviiland). *Acta Trop* 12:289–307
- Mikheyev A, Tschinkel W (2004) Nest architecture of the ant *Formica pallidefulva*: structure, costs and rules of excavation. *Insectes Soc* 51(1):30–36
- Noirot C, Noirot-Timothee C (1962) Construction et reconstruction du nid chez. *Cubitermes fungifaber*. *Symp Genet Biol Ital* 11:180–188
- Pie M, Rosengaus R, Traniello J (2004) Nest architecture, activity pattern, worker density and the dynamics of disease transmission in social insects. *J Theor Biol* 226(1):45–51
- Porta S, Crucitti P, Latora V (2006) The network analysis of urban streets: a dual approach. *Physica A* 369:853–866.
- R Development Core Team (2006). R: a language and environment for statistical computing. R foundation for statistical computing, Vienna (ISBN 3-900051-07-0)
- Strahler AN (1952) Dynamic basis of geomorphology. *Geol Soc Am Bull* 63:923–938
- Traniello FAJ, Rosengaus BR (1997) Ecology, evolution and division of labour in social insects. *Anim Behav* 53:209–213
- Tschinkel W (1998) Sociometry and sociogenesis of colonies of the harvester ant, *Pogonomyrmex badius*: worker characteristics in relation to colony size and season. *Insectes Soc* 45(4):385–410
- Tschinkel W (1999a) Sociometry and sociogenesis of colonies of the harvester ant, *Pogonomyrmex badius*: distribution of workers, brood and seeds within the nest in relation to colony size and season. *Ecol Entomol* 24(2):222–237
- Tschinkel W (1999b) Sociometry and sociogenesis of colony-level attributes of the florida harvester ant (hymenoptera: Formicidae). *Ann Entomol Soc Am* 92(1):80–89
- Tschinkel W (2004) The nest architecture of the florida harvester ant, *Pogonomyrmex badius*. *J Insect Sci* 4:1–19
- Turner JS (2000) *Extended organism: the physiology of animal-built structures*. Harvard University Press, Cambridge
- Williams DF, Lofgren CS (1988) Nest casting of some ground-dwelling Florida ant species using dental labstone. In: Trage JC (ed) *Advances in myrmecology*. Brill, Leiden, pp 433–443